

# Chapter 37

## The Marsh's Membrane: A Key-Role for a Forgotten Structure



Jean-Pierre Cuif and Yannicke Dauphin

**Abstract** Recent imaging methods applied to the growing edge of the *Pinctada margaritifera* shell allow for a better appreciation of ancient structural data. Growth of the *Pinctada* shell (both lateral extension and thickness increase) is a coordinated mechanism involving a series of clearly identified steps in contrast to the prevailing concept of a direct “self-assembly” process.

**Keywords** Periostracal transit · Flexible shell · Layered growth mode · Marsh membrane

### 37.1 Introduction

In contrast to Wada (1961) or Wilbur (1964) who recognized the importance of a specific structural phase predating the prismatic layer of mollusk shells (Fig. 37.1a), most modern investigators propose microstructural schemes in which the calcite prisms and their organic envelopes are directly and simultaneously produced at the growing edges of the shells (Saleuddin and Petit 1983; Volkmer 2007; Soldati et al. 2008). These models share the surprising ability of the prisms to continue to grow after having been covered by the nacreous layer. This is also the case in the scheme initiated by Petit (1978) and repeated up to Calvo-Iglesias et al. (2016, fig. 10) who summarized the concept of a remotely controlled formation of the prismatic layer: “Molecules secreted into the extrapallial cavity would be self-assembled and they reach the shell growing area without the participation of any cell.”

---

J.-P. Cuif (✉)

Centre de recherche sur la paléodiversité et les paléoenvironnements, CR2P – UMR 7207, Museum National d’Histoire Naturelle, Paris, France

Y. Dauphin

Institut de systématique, Evolution, Biodiversité, ISYEB – UMR 7205, Muséum national d’Histoire naturelle, Paris, France

e-mail: [Yannicke.dauphin@upmc.fr](mailto:Yannicke.dauphin@upmc.fr)

© The Author(s) 2018

K. Endo et al. (eds.), *Biom mineralization*,  
[https://doi.org/10.1007/978-981-13-1002-7\\_37](https://doi.org/10.1007/978-981-13-1002-7_37)

349

In such models, no place exists for the “innermost shell lamella” described by Marsh and Sass (1983) as “a single continuous layer which forms the inner surface of the shell ... firmly attached to the mineral in the underlying calcified layer”.

Here, through a microstructural approach of the growing edge of a prismatic shell layer, an attempt is made to establish a junction between the several decade-old observations clearly neglected in current literature.

## 37.2 Material and Methods

Adult pearl oysters (*Pinctada margaritifera*) were collected alive in Tuamotu archipelago. Young samples come from the hatchery of the Direction des Ressources Marines et Minières (DRMM, the Polynesian governmental office for pearl cultivation).

Observations were carried out with optical microscopy (natural and polarized light), scanning electron microscopy in both secondary and backscattered electron modes, and atomic force microscopy in tapping mode. X-ray diffraction measurements were performed at the ID13 beam line of the ESRF (Grenoble).

## 37.3 Results

### 37.3.1 Structure of the Flexible Shell Initiated and Developed in the Periostracal Groove

On the internal side of the periostracal film, numerous nonadjacent mineral disks are visible and regularly distributed (Fig. 37.1b, c). Every disk is growing around a non-mineralized center (Fig. 37.1d, arrows). The concentric mode of growth of the disks is visible of the outer side (Fig. 37.1e), whereas their inner side reveals a continuous granular structure (Fig. 37.1f). Using transmitted polarized light, the disks appear homogenous, each of them with a specific nuance always in the gray levels of the Newton scale (Fig. 37.1g). The single-crystal behavior of the disks is well

---

**Fig. 37.1** (continued) disks are clearly visible (**d**: arrows); Bar 30  $\mu\text{m}$  (**c**), 15  $\mu\text{m}$  (**d**). (**e**) Central nodule surrounded by concentric growth layers. Bar 8  $\mu\text{m}$ . (**f**) Granular appearance of the inner surface of a disk. Bar 6  $\mu\text{m}$ . (**g**) Optical view of disks (transmitted polarized light). Note the homogeneity of the gray levels for every disk. Bar 15  $\mu\text{m}$ . (**h–i**) Three series of nine points where X-ray diffraction was carried out on a single disk. Note the superposition of the diffraction spots (**i**). (**j–l**) Series of growing disks. Thickness does not increase during diametral growth; periostracum almost completely discarded excepted in left part of the picture. Bar 20  $\mu\text{m}$ . (**m**) The flexible shell at the end of the periostracal phase, just before passage to the rigid shell status. Note the 3  $\mu\text{m}$  thickness of the disks. Bar 50  $\mu\text{m}$ . (**n**) Scheme of a section of the shell growing edge cut perpendicularly to shell surface. Focus is made on the transit of the disks carried on the internal side of the periostracum, from deposition of the disk organic centers (*oc*) up to the upside-down movement (*ud*, arrow) by which the disks become the initial substrates for prism growth

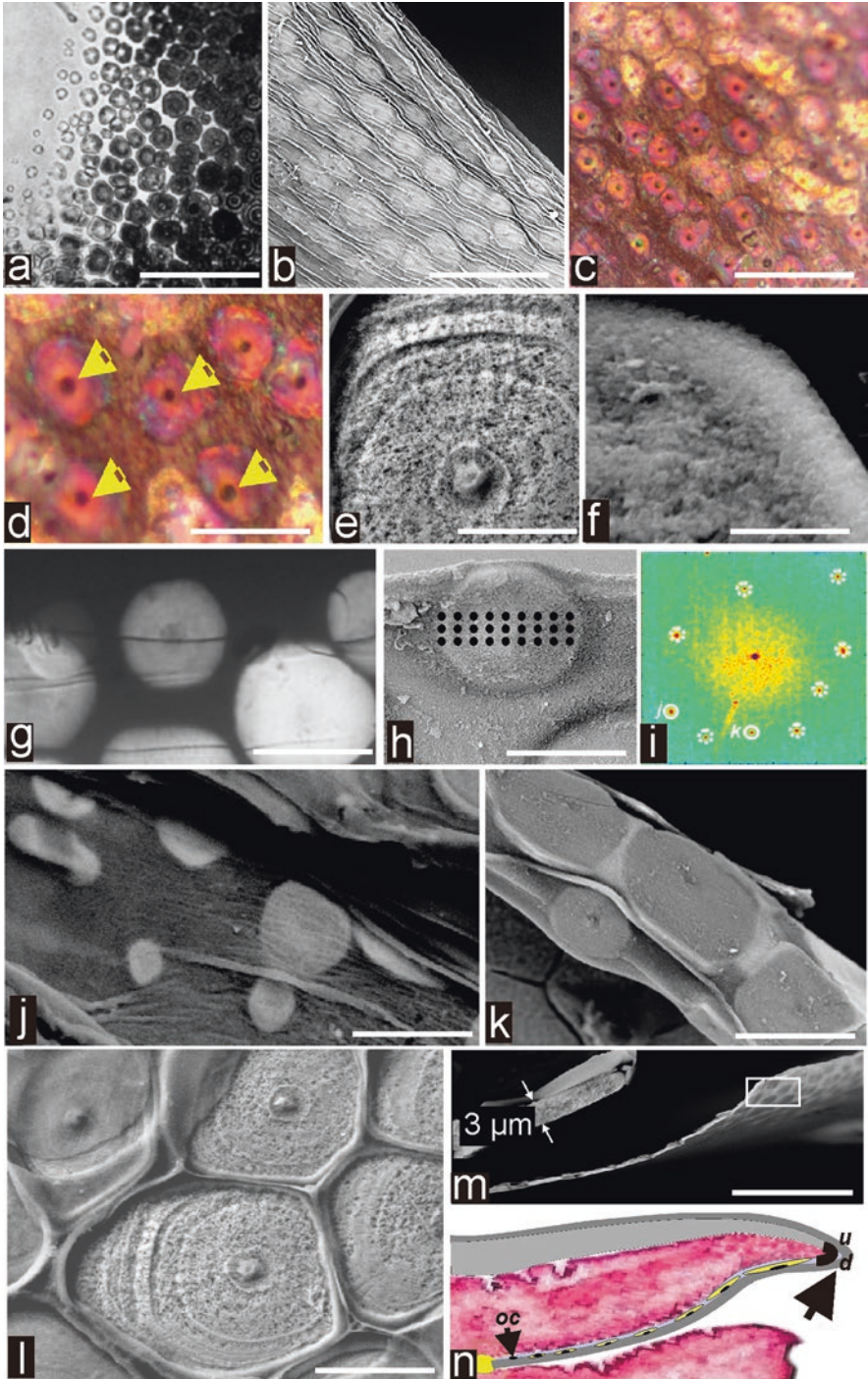


**Fig. 37.1** (a) Wada (1961) reprinted in Wilbur (1964). Growing edge surface of a *Pinctada fucata* shell viewed in transmitted polarized light. Bar 50  $\mu\text{m}$ . (b) SEM view of the outer surface of the periostracal membrane. Through the membrane the growing disks are visible. Note their centers. Bar 30  $\mu\text{m}$ . (c–d) Optical view of an equivalent area (episcopic polarized light). Centers of the

established by the perfect superposition of the spots in a series of 27 X-ray diffractions in a single disk (Fig. 37.1h, i). Through their concentric growth mode during their transportation by the periostracum acting as a conveyor belt, the disks reach their maximal size, becoming in close contact at the distal end of the periostracal groove (Fig. 37.1j–m). Their thickness remains about 3–4  $\mu\text{m}$  (Fig. 37.1m, n, black arrow).

### ***37.3.2 Transition from Flexible to Rigid Shell: Occurrence of a New Growth Mode***

The distal end of the periostracal transit is a turning point in shell formation. Through an upside-down movement, the disks are placed in geometrical continuity with the previously built “rigid shell.” By this movement, the internal sides of the disks (with non-mineralized centers) become the outer side of the shell growing edge. The outer surface of the shell growing edge shows the roughly circular crests, the dimensions of which correspond to the final stages of the discoid units developed in the “flexible shell” stage (Fig. 37.2a).

SEM view of the internal side in the same area reveals the polygonal morphology of the mineral building units (Fig. 37.2b) whose single crystal behavior is obvious in transmitted polarized light (Fig. 37.2c). Transition from discoid to polygonal morphology of the mineral units is well illustrated by transmitted polarized light (Fig. 37.2d). The limits of the previously discoid units are still visible (Fig. 37.2d: blue arrows), while the mineral phase has been extended up to become in contact to the neighboring units (Fig. 37.2d: red arrows). This close contact between the newly formed polygonal units ensures the shell rigidity.

This developmental step shows the first occurrence of an additional component of the shell: the internal side of the crystal-like polygonal units is now covered by a continuous organic membrane (Fig. 37.2b: Mm) so that the mineral phase is sandwiched between the external periostracum and this internal organic membrane. Simultaneously, a completely different biomineralization pattern can be observed. Instead of an individual lateral extension of the disks, mineralization occurs as a synchronic process insuring a simultaneous increase of shell thickness (Fig. 37.2e). Once more, the organic film is visible at the internal side of the polygonal units (Fig. 37.2e, arrows). It is still present (Fig. 37.2f, arrows) when the repeated layered growth process leads the thickness of these calcareous units to be superior to their lateral dimensions, justifying the term “prism.” Closer observations of the basal surface of the prisms leave no doubt about the presence of this well-individualized membrane (Fig. 37.2g, arrows). This membrane, permanently present at the internal surface of the prisms, exhibits a granular structure rather similar to the granular structure of the mineral phase of the prisms (Fig. 37.2h–j).

## 37.4 Discussion

### 37.4.1 *Inadequacy of the “Direct Crystallization” Model to Account for Formation of the Prismatic Layer in the Pinctada Shell*

The “molecular self-assembly process” underlying recent schemes and explicitly formulated by Calvo-Iglesias et al. (2016) cannot be applied to the outer shell layer of the *Pinctada margaritifera*. The two-phase mechanism briefly described in the present report was suggested by Wada (1961, Figure 8) and Wilbur (1964, Figure 10), who observed circular crystalline units growing “in oolitic aggregation” becoming progressively polygonal by mutual contact. The crystalline properties of the mineral units forming the “flexible shell” were established by Suzuki et al. (2013), but the presence of a non-mineralized center in each of these calcareous units basically modifies the interpretation of their formation and role.

### 37.4.2 *Origin of the Crystallographic Individuality of the Calcite Prisms of the Pinctada Shell*

From the deeper parts of the periostracal groove, the calcareous disks transported on the internal side of the periostracum exhibit a non-mineral center, suggesting that this organic glomerule was deposited in close vicinity to the group of cells dedicated to the formation of the periostracum itself (see histological sections in Jabbour et al. 1992). Polarization microscopy and multiple X-ray diffractions show that, in conformity to the results of Suzuki et al. (2013), the disks are crystal-like units, each of them with a specific crystalline orientation (assessed by the distinct gray levels corresponding to a 3–4  $\mu\text{m}$  thickness measured by SEM; Fig. 37.1m). It can be assumed that these specific crystalline orientations take origin in the slightly diverse orientations of the organic substrates of the disks.

From this very early origin of crystallographic orientation in the transitional phase from flexible to rigid shells (Fig. 37.2d), the crystallographic orientation of the first mineral polygons forming the rigid shell relies on the crystallographic orientation of the disks after their upside-down movement. In further growth steps of the prisms, crystallographic orientation of every newly formed polygon is repeated.

Thus, conclusion arises that the long-recognized crystal-like behavior of the prisms forming the outer shell layer of the *Pinctada* is determined in the deeper part of the periostracal groove and is by no means the result of a “self-assembly process.”

### 37.4.3 *The Crystal-Like Disks as Examples of Non-Ion-by-Ion Crystallization*

In the search of evidences for a biological control of crystallization, we must note that all along their growth, the freely and independently crystallizing disks exhibit a concentric layering as obvious traces of their stepping growth mode. If disk crystallization was based on an ion-by-ion mechanism, the presence of calcite faces oriented in conformity with those of crystals produced by purely chemical precipitation should appear in these distant and freely growing units. This is not the case: no exception has been observed to the circular morphology and concentric mode of growth for the crystal-like units. This provides a contrario evidence for a nonionic but biochemically controlled mode of crystallization (i.e., non-purely chemical).

### 37.4.4 *The Marsh's Membrane as Coordinator of the Layered Growth Mode of the Prisms*

Occurrence of the organic membrane covering the newly formed polygons (Fig. 37.2e) and its persistency during further development of the prisms introduce a new factor to be taken into account in the crystallization process. Its granular structure was noted from the early descriptions (Fig. 37.2k) and among the very rare mentions that have been made of this shell component. Yan et al. (2008) have well noted the time-based variability in the development of these grains, leading these authors to qualify the Marsh's membrane as a "dynamic structure." This means that the Marsh's membrane is involved in the mineralization process, a conclusion here confirmed (Fig. 37.2g–j) and by previous observations (Cuif et al. 2014).

One of the most striking features of the calcite prisms in *Pinctada margaritifera* is the microstructural change that regularly occurs after about 150  $\mu\text{m}$  growth length. After an initial stage with a single crystal structure (Fig. 37.2l), the prisms become polycrystalline (Fig. 37.2m) (Cuif et al. 2011, 2014; Checa et al. 2013).

---

**Fig. 37.2** (continued) the front raw and the changing colors revealing the increasing thickness of the polygonal units. Bar 50  $\mu\text{m}$ . (d) Formation of the rigid shell: limits of the disks, still visible by the round-shaped trace (blue arrows), are overcome by new mineral deposits that bring the neighbor units in close contact (red arrows). Transmitted polarized light; Bar 20  $\mu\text{m}$ . (e) The Marsh's membrane is visible at the base of the newly formed polygons (arrows). Note the decayed perios-tracum making visible the outer surface of the initial disks and their centers. Bar 10  $\mu\text{m}$ . (f) The Marsh's membrane at the inner surface of young prisms. Compare to picture of the compartment lamella by Bevelander and Nakahara (1980). Bar 25  $\mu\text{m}$ . (g) Closer view of the Marsh's membrane. Note the transversal striation and the granular structure. Bar 5  $\mu\text{m}$ . (h–j) Aspect of the Marsh's membrane: h, SEM view, Bar, 5  $\mu\text{m}$ ; i, SEM view, Bar, 2  $\mu\text{m}$ ; j, AFM view, Bar, 150 nm. (k) Reprint of a Marsh figure (TEM). Note the granular pattern of the Marsh membrane, corresponding to the high-resolution SEM view here reported. Bar: 0.5  $\mu\text{m}$ . (l–m) Thin sections (transmitted polarized light) in the upper part of prisms (up to 150  $\mu\text{m}$ ) and in their lower part. Note the passage from single crystal-like to polycrystalline organization. Bar: 50  $\mu\text{m}$  (l) and 30  $\mu\text{m}$  (m)

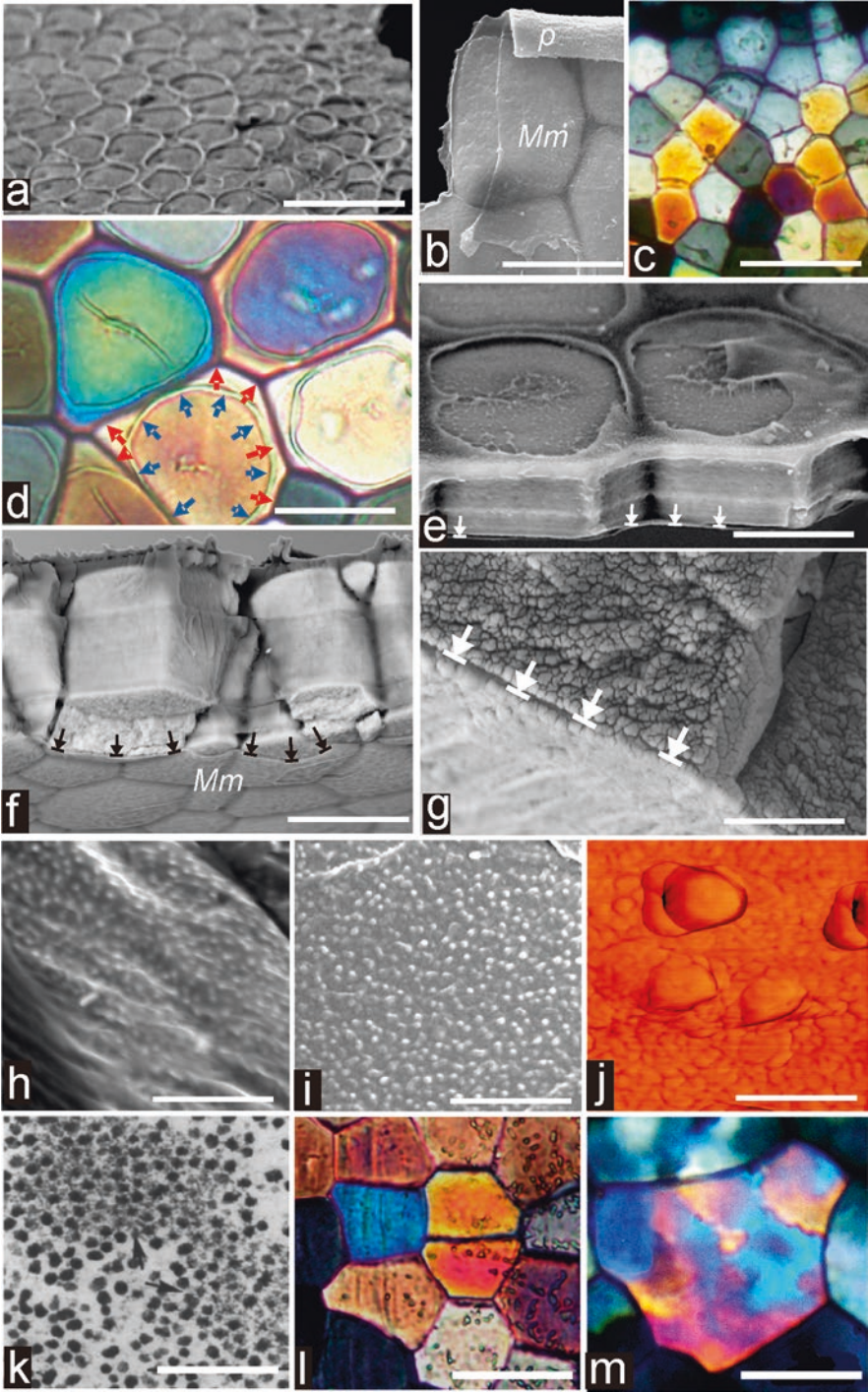


**Fig. 37.2** (a) SEM view of the outer surface of the rigid shell at its growing edge. Bar 30  $\mu\text{m}$ . (b) Internal side of a polygonal unit at the distal row of the rigid shell. Mm: organic membrane. SEM view, Bar 25  $\mu\text{m}$ . (c) Polygonal units in transmitted polarized light. Note the various gray levels in

Such a coordinated change contradicts the theory of “crystal growth competition” that postulates a selection of the best oriented crystals leading to a progressive increase of the mean diameter in a given shell.

### 37.4.5 *The Key Role of the Marsh’s Membrane in Microstructural Evolution of the Prisms*

*Pinctada* calcite prisms are submitted to microstructural changes during aging (Cuif et al. 2014), and composition of both the mineral and organic phases is modified before the occurrence of nacre deposition (Cuif et al. 2011). Microstructural variations of the prisms during shell growth provide evidence for time-based genetically programmed secretion process.

What is remarkable is that the repeated back-and-forth movements of the mantle due to the rhythmic mode of life of the animal leave no trace in prism microstructure. This contrast epitomizes the key role of the Marsh’s membrane in shell formation. When the animal withdraws its mantle for shell closure, the Marsh’s membrane stays in place at the basis of the prismatic layer. Thus, when the mantle returns to an actively mineralizing position, growth of the microstructural units (each of them with its specific crystalline orientation) can restart without any apparent interruption.

Under many respects understanding the Marsh’s membrane as an active interface between mantle secretions and shell is an important issue for both microstructural analysis and any attempt to create biomimetic materials.

## References

- Bevelander G, Nakahara H (1980) Compartment and envelope formation in the process of biological mineralization. In: Omori M, Watabe N (eds) The mechanisms of biomineralization in animals and plants. Tokai University Press, Kanagawa
- Calvo-Iglesias J, Pérez-Estévez D, Lorenzo-Abalde S, Sánchez-Correa B, Quiroga María I, Fuentes José M, González-Fernández A (2016) Characterization of a monoclonal antibody directed against *Mytilus spp.* larvae reveals an antigen involved in shell biomineralization. PLoS One 11:1–17. <https://doi.org/10.1371/journal.pone.0152210>
- Checa AG, Bonarski JT, Willinger MG, Faryna M, Berent K, Kania B, Gonzalez-Segura A, Pina CM, Pospiech J, Morawiec A (2013) Crystallographic orientation inhomogeneity and crystal splitting in biogenic calcite. J R Soc Interface 10:20130425
- Cuif JP, Dauphin Y, Sorauf JE (2011) Biominerals and fossils through time. Cambridge University Press, Cambridge, 490 p
- Cuif JP, Burghammer M, Chamard V, Dauphin Y, Godard P, Le Moullac G, Nehrke G, Perez-Huerta A (2014) Evidence of a biological control over origin, growth and end of the calcite prisms in the shells of *Pinctada margaritifera* (Pelecypod, Pterioidea). Minerals 4:815–834
- Jabbour-Zahab J, Chagot D, Blanc F, Grizel H (1992) Mantle histology, histochemistry and ultrastructure of the pearl oyster *Pinctada margaritifera* (L.). Aquat Living Resour 5:287–298



- Marsh ME, Sass RL (1983) Calcium-binding phosphoprotein particles in the extrapallial fluid and innermost shell lamella of clams. *J Exp Zool* 226:193–203
- Petit H (1978) Recherches sur des séquences d'évènements périostraux lors de l'élaboration de la coquille d'*Amblyema plicata* Conrad, 1834. Thèse, Laboratoire de Zoologie, Université de Bretagne occidentale, 276 pp
- Saleuddin ASM, Petit H (1983) The mode of formation and the structure of the periostracum. In: Saleuddin ASM, Wilbur KM (eds) *The Mollusca*. Academic, New York
- Soldati AL, Jacob DE, Wehrmeister U, Hofmeister W (2008) Structural characterization and chemical composition of aragonite and vaterite in freshwater cultured pearls. *Mineral Mag* 72:577–590
- Suzuki M, Nakayama S, Nagasawa H, Kogure T (2013) Initial formation of calcite crystals in the thin prismatic layer with the periostracum of *Pinctada fucata*. *Micron* 45:136–139
- Volkmer D (2007) Biologically inspired crystallization of calcium carbonate beneath monolayers: a critical overview. In: Behrens P, Baeuerlein E (eds) *Handbook of biomineralization: biomimetic and bioinspired chemistry*. Wiley, Hoboken
- Wada K (1961) Crystal growth of molluscan shells. *Bull Natl Pearl Res Lab* 36:703–782
- Wilbur KM (1964) Shell formation and regeneration. In: Wilbur KM, Owen G (eds) *Physiology of mollusca*. Academic, New York
- Yan Z, Ma Z, Zheng G, Feng Q, Wang H, Xie L, Zhang R (2008) The inner shell-film: an immediate structure participating in Pearl Oyster formation. *Chembiochem*. <https://doi.org/10.1002/CBC.200700553>

**Open Access** This chapter is licensed under the terms of the Creative Commons Attribution 4.0 International License (<http://creativecommons.org/licenses/by/4.0/>), which permits use, sharing, adaptation, distribution and reproduction in any medium or format, as long as you give appropriate credit to the original author(s) and the source, provide a link to the Creative Commons license and indicate if changes were made.

The images or other third party material in this chapter are included in the chapter's Creative Commons license, unless indicated otherwise in a credit line to the material. If material is not included in the chapter's Creative Commons license and your intended use is not permitted by statutory regulation or exceeds the permitted use, you will need to obtain permission directly from the copyright holder.

